Sizing and simulating geothermal bore fields using thermal response factors

Michel Bernier, Professor, Département de génie mécanique, Polytechnique Montréal, Montréal, Québec, Canada

Abstract: This paper summarizes the state-of-the art of geothermal bore fields design and simulation using thermal response factors. In the first part of the paper, the concept of thermal response factors, also known as g-functions, is examined. It is shown that the ratio of buried depth to borehole height should be considered as it becomes important for short boreholes. Results obtained with an analytical technique to obtain g-functions are presented and the effects of using different types of borehole wall boundary conditions are analyzed. Then, a procedure to size bore fields based on g-functions is presented. The procedure involves iterative calculations where g-functions are evaluated as the solution proceeds. Finally, the basic equations to perform annual simulations of bore fields are presented and the concepts of temporal superposition and load aggregation are reviewed.

Key Words: borehole, sizing, simulation, thermal response factors, g-function

1 INTRODUCTION

Ground-coupled heat pump (GCHP) systems have seen their popularity grow over the last two decades because of their potential to reduce energy consumption in both heating and cooling applications. A typical GCHP system is presented schematically in Figure 1. It consists of a series of heat pumps connected to a fluid loop and a series of ground heat exchangers which form a bore field. Heat pumps either collect or reject energy in the fluid loop. The sum of all the individual heat exchanges with the fluid loop corresponds to the amount of power that will be collected or rejected into the ground during a time period. When connected in parallel in a two-pipe system (as shown in Figure 1), heat pumps have the same inlet fluid temperature ($T_{in,HP}$ in Figure 1) and each borehole as the same inlet temperature ($T_{out,HP}$ in Figure 1).

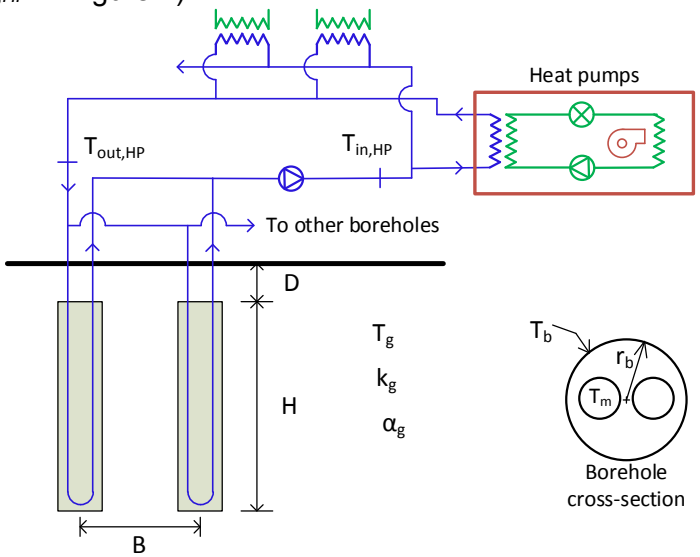


Figure 1: Schematic representation of a typical GCHP system

The heat exchange between the borehole wall and the ground depends on the thermal conductivity, k_g, and thermal diffusivity, α_g, of the ground as well as ground temperature, T_g. The bore field is characterized by the number of boreholes (*nb*), the borehole radius (r_b), the height of each borehole (H), the buried depth (D), and the borehole spacing (B).

It is common to separate the regions inside and outside the boreholes and solve the heat transfer problem for each region separately. In this paper, only transient heat transfer in the ground outside the borehole is considered. Heat transfer inside the borehole is treated as a steady-state process with an equivalent borehole thermal resistance, R_b, between the mean fluid temperature in the borehole, T_m, and the borehole wall temperature, T_b.

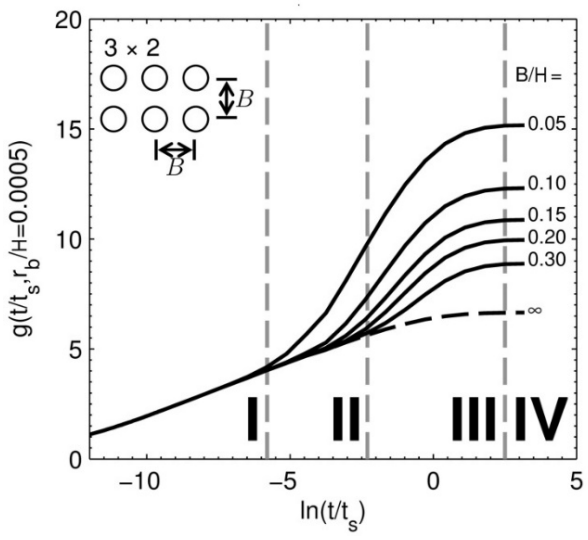
2 THERMAL RESPONSE FACTORS

2.1 Eskilson's original work

The pioneering work of Eskilson is at the origin of thermal response factors, also known as g-functions (Eskilson, 1987). As stated in the beginning of his thesis the purpose of his work was relatively simple: "*The aim of our studies is to obtain formulas for the relation between the heat extraction rate q and the required borehole temperature* T_b". He proposed to relate T_b to the heat transfer rate per unit length, q, with the following equation:

$$T_b = T_g - \frac{q}{2\pi k_g} \cdot g(t/t_s, r_b/H, B/H) \quad (1)$$

where g represents the g-function. As shown in Equation 1, Eskilson established that g-functions depend on three non-dimensional parameters: B/H, the ratio of the borehole spacing over the borehole length; r_b/H, the ratio of the borehole radius over the borehole length; and t/t_s , a non-dimensional time where t_s is a characteristic time (= $H^2/9\alpha_g$). g-functions curves are presented graphically on Figure 2 for a 3×2 bore field as a function of $\ln(t/t_s)$ for six bore field spacings (B/H) and for a particular value of r_b/H (=0.0005). The curve for B/H = ∞ corresponds to the g-function of a single borehole (with r_b/H = 0.0005). These non-dimensional curves are universal and apply to any 3×2 bore field. The Table in Figure 2 shows a numerical example with two geometries that have identical values of B/H and r_b/H but different values of B, H, and r_b. For $\ln(t/t_s)$ = -2.3 (i.e. t/t_s = 0.1) and α_g = 0.1 m²/day, the g-function is equal to 10 for both geometries. Finally, if it is assumed that T_g = 0°C, k_g = 1.0 W/m-K, and q = -6.28 W/m (heat injection), then T_b = 10°C. This borehole temperature will be reached at t = 3.04 years for geometry A and t = 6.85 years for geometry B.



Geometry	A	B
Size	3 × 2	3 × 2
B (m)	5	7.5
H (m)	100	150
r_b (m)	0.05	0.075
B/H	0.05	
r_b/H	0.0005	
$ln(t/t_s)$	-2.3	
g	10 (from figure on the left)	
α_g (m²/day)	0.1	
t_s (years)	30.4	68.5
t (years)	3.04	6.85
k_g (w/m²)	1.0	
T_g (°C)	0	
q (W/m²)	-6.28 (set to $-2\pi k_g$)	
T_b (°C)	10	

Figure 2: Six g-functions curves for a 3 x 2 bore field with r_b/H=0.0005 (left). Example on the use of g-function curves for two geometries (right).

As indicated in Figure 2, four different thermal regions can be identified on a g-function curve. In region I, all curves merge into one linear curve. Heat transfer can be considered to be one-dimensional (in the radial direction) and boreholes have not started to interact with each other. The starting point of region II is specific to each bore field configuration and to a particular *B/H* ratio. For the geometry shown in Figure 2 and for *B/H* = 0.05, region II starts at $\ln(t/t_s) \approx -5.5$ where the g-function curve diverges form the g-function of a single borehole and boreholes start to thermally interact with each other. This thermal interaction continues in regions III and IV. Region III starts when $t > 0.1t_s$ (i.e. $\ln(t/t_s) > -2.3$). According to Eskilson (1987), this is the time when heat transfer near boreholes becomes two-dimensional (radial and axial). Finally, the fourth region is characterized by a plateau where g-functions reach their "steady-state" values at $\ln(t/t_s) > 2.5$.

It should be noted that g-functions are presented for a given r_b/H ratio. It is possible to correct g-functions for other r_b^*/H ratio using (Eskilson, 1987):

$$g_2(t/t_s, r_b^*/H) = g_1(t/t_s, r_b/H) - \ln\left[\frac{r_b^*/H}{r_b/H}\right] \quad (2)$$

where g_2 is the corrected g-function and g_1 is the g-function obtained with r_b/H . For example, for a bore field similar to geometry A in Figure 2 but with r_b^* = 0.06 m, then the corrected g-function would be:

$$g_2 = 10 - \ln\left(\frac{0.0006}{0.0005}\right) = 10 - 0.18 = 9.82 \quad (3)$$

Eskilson evaluated g-functions for a number of configurations using a buried depth (*D*) of 4-5 m. These values were chosen after numerical simulations on long boreholes that showed only small variations of the borehole wall temperature for buried depth of 2-8 m. However, for short boreholes, the buried depth becomes important as illustrated in Figure 3. In this figure g-functions are presented for a 6×4 bore field of height *H* = 5 m and radius r_b = 0.05 m with a borehole spacing *B* = 1 m. The g-function curves are significantly different as *D* is varied. For example, in region IV when "steady-state" is reached, the g-functions vary from ≈ 12 to ≈ 20 when the *D/H* ratio is varied from 0 to 1. Thus, for completeness, the definition of the g-function should be expanded to include *D/H* as the fourth non-dimensional parameter:

$$T_b = T_g - \frac{q}{2\pi k_g} \cdot g(t/t_s, r_b/H, B/H, D/H) \quad (4)$$

Finally, if the borehole thermal resistance, R_b, is known then the mean fluid temperature in the borehole is given by:

$$T_m = -qR_b + T_b \quad (5)$$

or

$$T_m = T_g - q(R_b + \frac{g}{2\pi k_g}) \quad (6)$$

It is also worth noting that g-functions of short boreholes reach their steady-state values more rapidly than for long boreholes. As shown by the top x-axis in Figure 3, "steady-state" is reached after ≈ 10 years for these 5 m long boreholes. In contrast, the 100 m long boreholes in geometry A (Figure 2) reach their plateau after ≈ 350 years.

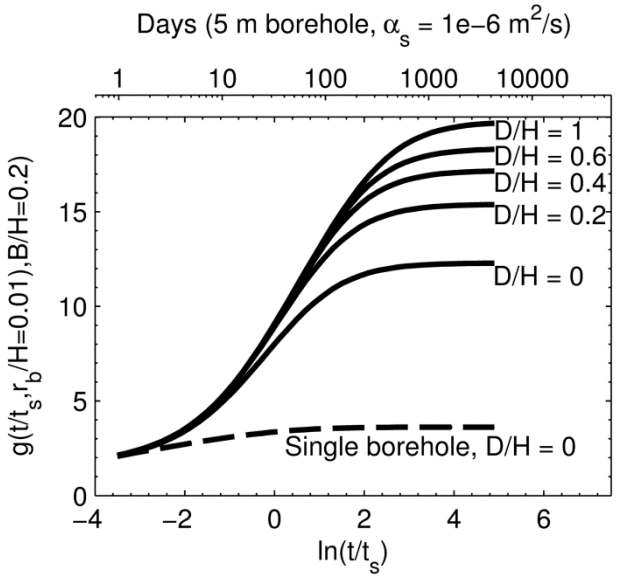


Figure 3: g-functions for various buried depth to height ratios (*D/H*) for a 6×4 bore field with *H* = 5 m, *B* = 1 m, and r_b = 0.05 m.

The four regions identified earlier for long boreholes (Figure 2) are positioned differently along the x-axis for short boreholes. In the case of Figure 3, axial effects (identified earlier as region III and which start at $\ln(t/t_s) = -2.3$) occur after only 3 days, a time similar to the occurrence of thermal interactions between boreholes, which occur after approximately 2 days.

2.2 Extension to short-time steps

Eskilson's original g-functions started at times corresponding to $\ln(t/t_s) \approx -4$. For typical boreholes this means that they are valid for relatively long-time steps of the order of one month. Yavuzturk and Spitler (1999) extended Eskilson's g-functions for shorter time steps. They also included the grout and pipe thermal resistance and thermal capacitance in their analysis. The authors subtracted the contribution of the steady-state thermal resistance of the borehole to the thermal response in order to follow Eskilson's definition of the g-functions.

2.3 Numerical and analytical determination of g-functions

Eskilson (1986) evaluated g-functions numerically using the finite difference method applied to a single borehole. He used a two-dimensional (radial-axial) mesh with fine grids near important thermal gradients, i.e. near borehole extremities and close to the borehole wall. Using the technique of images, the temperature field around the borehole is superimposed to a symmetric temperature field with temperatures of opposite sign, taking the ground surface as the axis of symmetry. Finally, for bore fields composed of more than one borehole, the numerical thermal response obtained for a single borehole is superimposed in space to account for thermal interaction among boreholes. As noted by Cimmino and Bernier (2014), this type of spatial superposition using numerical solutions can lead to inaccurate g-functions for large aspect ratio bore fields if the radial mesh is too coarse.

One often overlooked aspect of g-functions is the borehole wall boundary condition that can be used to generate them. Cimmino and Bernier (2014) have characterized three possible boundary conditions referred to as BC-I, BC-II, and BC-III. These boundary conditions are shown schematically in Figure 4. Unequal borehole lengths are shown in Figure 4 to keep the analysis general.

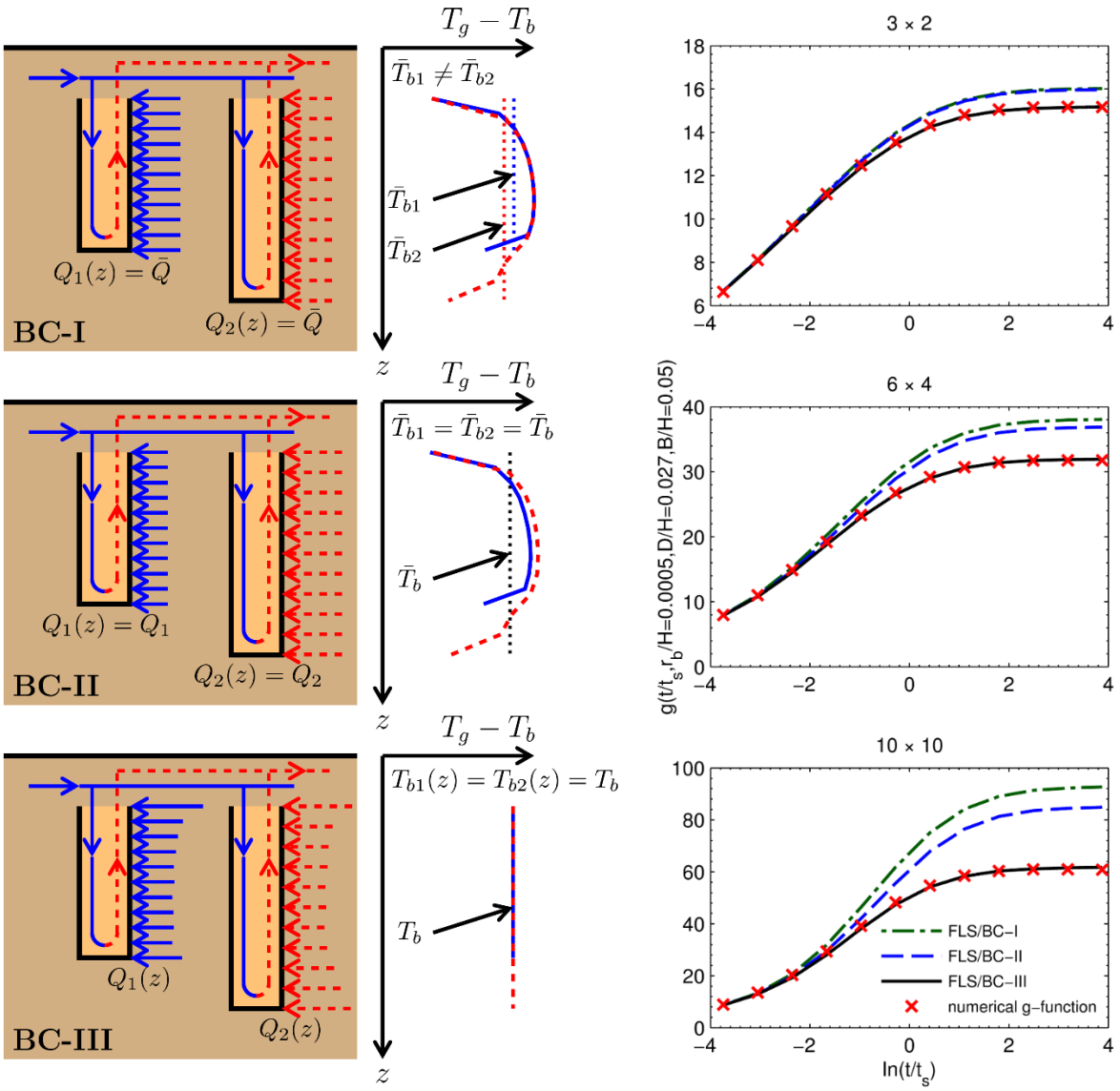


Figure 4 (left): Three possible boundary conditions to obtain g-functions (Cimmino and Bernier, 2014).
Figure 5 (right): Comparison between analytical g-functions based on the finite line source (for three different boundary conditions) and numerically generated g-functions (Cimmino and Bernier, 2014).

In the first boundary condition (BC-I) the heat extraction rate (*Q*) is uniform along the length of the boreholes and these rates are equal for all boreholes. As indicated in the temperature profile graph along the BC-I drawing in Figure 4, this boundary condition leads to different average borehole wall temperatures in the bore field. For BC-II, the average borehole wall temperature is the same for all boreholes and the heat extraction rates are uniform along the borehole length. However, the heat extraction rates are different for each borehole. Finally, the third boundary condition imposes a uniform borehole wall temperature along the length of the boreholes and this borehole wall temperature is equal for all boreholes. This leads to non-uniform heat extraction rates along the length of the borehole and different heat extraction rates among boreholes. The solution complexity and the computational time increases from BC-I to BC-III. Cimmino and Bernier (2014) report that g-functions calculated using BC-I and BC-II require approximately the same calculation time. However, the calculation time using BC-III is one order of magnitude greater than for BC-I/BC-II. Finally, it should be noted that Eskilson used BC-III to obtain his g-functions (Claesson, 2013).

It is possible to generate thermal response factors using analytical solutions to transient heat transfer in the ground. One possible approach is to use the infinite cylindrical heat source (CHS) for small times and then use the two-dimensional (axial and radial) finite line source (FLS) solution for longer times (Cimmino et al., 2103). Philippe et al. (2009) present validity limits for these analytical solutions and it is shown that, for typical conditions, the CHS should be used for times less than a few days.

Calculations involving the CHS can easily be implemented using the techniques proposed by Cooper (1976) or Baudoin (1988). When the FLS solution is used to obtain the average borehole wall temperature over a certain borehole length, calculations involve a double integral. Lamarche and Beauchamp (2007) and Claesson and Javed (2011) have provided relatively simple ways to convert the double integrals into single integrals to reduce the calculation time.

Cimmino and Bernier (2014) have derived g-functions analytically using the FLS and appropriate spatial and temporal superposition. The boreholes can be placed into irregular patterns (different borehole spacings) and can also have different individual lengths. The methodology is implemented into MATLAB with a convenient graphical user interface which pre-processes the hourly values of the thermal response factors for use in energy simulation programs (Cimmino and Bernier, 2013).

Cimmino and Bernier (2014) compared the resulting g-functions against those determined numerically. This comparison is shown in Figure 5 for three different bore field configuration and the three boundary conditions identified earlier. First, it should be noted that all four curves merge into a single curve for small values of $\ln(t/t_s)$. Thus, for small times, g-functions could be calculated using BC-I which is relatively simple to implement. Secondly, the g-functions determined with the FLS/BC-III approach are almost identical to those calculated numerically with the original methodology of Eskilson indicating that the analytical method developed by Cimmino and Bernier (2014) is accurate.

3 SIZING OF GEOTHERMAL BORE FIELDS

3.1 Simple sizing example

One simple starting point for sizing bore fields is to assume that there is no borehole thermal interference and that axial heat transfer effects near the borehole extremities are negligible. With these assumptions, a simple calculation using the CHS will lead directly to the borehole length. Philippe et al. (2010) presented a simple spreadsheet to accomplish this task. Then, it is possible to look at the length changes caused by axial effects by examining the g-function for an infinite borehole spacing (curve for B/H = ∞ in Figure 3). Finally, the effects of borehole thermal interference on the borehole length can be quantified by selecting a bore field configuration and borehole spacing. The impact of these various assumptions are best described with an example as shown Table 1. In this example, a constant amount of power (9.63 kW) is injected into the bore field. The total borehole length required to have a mean fluid temperature of 35°C after 20 years is to be determined. The other parameters are listed at the bottom of Table 1.

As shown in Table 1, the total length is equal to 312 m when axial effects and borehole thermal interaction are not considered. This evaluation is based on the CHS solution as determined using a technique described by Bernier (2000).

If a 3×2 bore field is to be installed and if it is assumed that the borehole spacing is high enough such that B/H -> ∞, then the total borehole length is reduced to 275.4 m (6 boreholes of 45.9 m each). Thus, axial effects which are taken into account in g-functions, have a

positive effect as they tend to reduce the required borehole length. In other words, enhanced heat transfer per unit length near the borehole extremities reduces the borehole length required for a given amount of heat injection. The final borehole length is obtained through iterative calculations. Based on a guess value of H (the value obtained with the CHS is a good first guess), Equation 6 is solved to obtain the g-function and the corresponding value of $\ln(t/t_s)$ on the $B/H \rightarrow \infty$ curve in Figure 3. Finally, using the definition of t_s , it is possible to find H. However, the g-function in Figure 3, correspond to a ratio r_b/H=0.0005. Thus, the g-function has to be corrected according to Equation 2 which leads to new values of $\ln(t/t_s)$ and H. The process is repeated until the value of H converges.

When boreholes are spaced 5 m apart, the total length required is 600 m as shown in the last column of Table 1. This value is obtained through iterations using the g-function curves (Figure 3). First, a borehole height H is assumed (the value obtained for B/H -> ∞ is a good first guess). Then, t_s, $\ln(t/t_s)$, and the corresponding g-function are evaluated. Finally, using Equation 6, the resulting value of T_m is calculated. If it corresponds to the limit set for T_m, iterations are stopped and the final borehole length is evaluated, if not calculations are repeated until convergence. In conclusion, thermal interaction is this example is significant as it increases the required length by a factor of about 2.

Table 1: Example showing the impact of three different calculation methods to evaluate the total borehole length

Evaluated with the CHS (axial effects and borehole thermal interactions are not considered)	Evaluated with g-function for 3x2 with B/H -> ∞ (borehole thermal interactions are not considered)	Evaluated with g-function for 3x2 and B = 5m
312 m	6 x 45.9 m = 275.4 m	6 x 100 m = 600 m
Parameters used for these calculations: r_b = 0.05 m; α = 0.1 m^2/day; T_g = 0°C; k_g = 1 W/m-K; q = -9.63 kW; t = 20 years; T_m = 35°C, R_b =0.1 m-K/W		

3.2 Bore field sizing equation

It is important to properly size bore fields to reduce drilling costs and avoid operational problems. The calculation procedure presented in the previous section cannot be generally applied as bore fields are usually not subjected to constant heat injection (or extraction). One popular approach recommended by ASHRAE (ASHRAE, 2011) is to use three consecutive thermal pulses. These pulses typically correspond to 10 to 20 years of yearly averaged heat load (q_y), followed by the peak average monthly ground load (q_m) and the peak hourly load (q_h) applied for a duration of 4 to 6 hours. The ASHRAE equation does not use g-functions. It is relatively simple to implement and does not require an iterative process. However, its accuracy, especially for long-term borehole thermal interference, has been questioned (Bernier et al., 2008).

Recently, Ahmadfard and Bernier (2014) proposed to modify the ASHRAE equation so that it can be based on g-functions:

$$L = \frac{q_h R_b + q_y R_{gy} + q_m R_{gm} + q_h R_{gh}}{T_m - T_g} \quad (6)$$

where L is the required borehole length (L = nb × H, where nb is the number of boreholes). The first term in the numerator accounts for heat transfer (assumed to be in steady-state) in the borehole from the fluid to the borehole wall where R_b is the borehole thermal resistance. The next three terms in the numerator account for transient heat transfer in the ground. These three terms are three consecutive ground thermal pulses multiplied by their respective

effective ground thermal resistances R_{gy}, R_{gm}, and R_{gh}. When based on g-functions, the values of R_{gy}, R_{gm}, and R_{gd}, take the following forms:

$$R_{gy} = \left(g_{(t_f)} - g_{(t_{f-t_1})}\right)/2\pi k_g\,,\ R_{gm} = \left(g_{(t_{f-t_1})} - g_{(t_{f-t_2})}\right)/2\pi k_g,\ R_{gh} = g_{(t_{f-t_2})}/2\pi k_g \qquad (7)$$

where $g_{(t_x - t_y)}$ is the g-function evaluated at ln((t_x-t_y)/t_s) for a given bore field and r_b/H and B/H ratios. The times t_1, t_2, and t_f correspond, typically, to 3650, 3680, and 3680.25 days, respectively.

It is to be noted that the determination of L (i.e. $nb \times H$) is an iterative process as R_{gy}, R_{gm}, and R_{gd} depend on L which is unknown *a priori.* Thus, software tools are often required to accomplish this task (e.g. Hellström and Sanner (1994), Spitler (2000)). These tools usually have a database of pre-calculated g-function values similar to those presented in Figure 2. Aside from the iterative process, the calculation procedure typically involves a correction factor (Equation 2) to account for different r_b/H ratios and an interpolation between B/H curves.

Ahmadfard and Bernier (2014) proposed a procedure that eliminates the need for Equation 2 and the interpolation between B/H curves. This procedure takes advantage of the FLS-based technique introduced by Cimmino and Bernier (2014) to calculate the required g-function with the correct r_b/H and B/H ratios. Thus, g-functions are evaluated "on the fly" during the iterative calculations. The whole g-function curve does not need to be evaluated as only three points are required. This process is illustrated in Figure 6 for a particular sizing problem (see Ahmadfard and Bernier (2014) for more details) with t_1 = 3650 days, t_2 = 3680 days, and t_f = 3680.25 days. The process starts with an initial guess for H. Then t_s is calculated and three values of the g-function are evaluated using Equation 7 for three corresponding values of ln((t_x-t_y)/t_s). These three points are indicated in the top curve in Figure 6 (the whole g-function curve is shown as a dotted line only for illustrative purposes). Equation 7 and 6 are then used to obtain a new estimate of L and H. The process is repeated and leads to three new g-function values which are shown on the bottom curve in Figure 6. Finally, a third iteration confirms the results of the second iteration as the three new points are exactly at the same location as the previous three points in Figure 6.

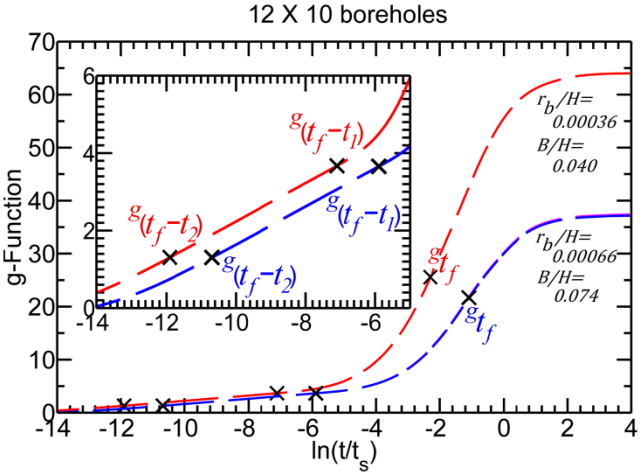


Figure 6: Illustration of the iterative process involved in solving Equation 6 (Amahfard and Bernier, 2014).

4 SIMULATION OF GEOTHERMAL BORE FIELDS

Once the bore field has been sized, its g-function curve can be calculated and used to determine the thermal response; it does not need to be recalculated during simulations. The

estimation of the heat pump energy consumption of a GCHP system requires simulations with a relatively short time step, usually one hour (or less). Typically, the heat transfer per unit length, q, in a bore field in a given time step depends on the building load and on the heat pump Coefficient of Performance (COP). In turn, the COP depends on the return fluid temperature from the bore field, $T_{in,HP}$ (Figure 1). Thus, iterations are generally required to obtain q. Once q is known, the g-function curve can be used to determine $T_{in,HP}$ and the heat pump COP.

Many energy simulation programs have a g-function based routine to evaluate $T_{in,HP}$ as a function of time (e.g. Fisher et al., 2006, Liu, 2008). Even though these programs may implement g-functions differently, they have the same basic approach which involves two major strategies: temporal superposition and load aggregation.

4.1 Temporal superposition

Temporal superposition was used earlier in conjunction with the evaluation of the effective ground thermal resistances (Equation 7) for borehole sizing. In fact, the borehole sizing equation 6 is a good starting point to explain how to perform energy simulations. Given that the borehole length is known, the sizing equation can be rearranged to give the mean fluid temperature :

$$T_m = T_g - \left[\frac{Q_1(g_{(t_3-0)}-g_{(t_3-t_1)})+Q_2(g_{(t_3-t_1)}-g_{(t_3-t_2)})+Q_3 g_{(t_3-t_2)}}{2\pi k_g L} + \frac{Q_3 R_b}{L}\right] \quad (8)$$

with $T_m = \frac{T_{in,HP}+T_{out,HP}}{2}$

In this equation, T_m is evaluated after three consecutive ground heat transfer rates, Q_1, Q_2, and Q_3, which are applied over three consecutive time intervals (0 to t_1, t_1 to t_2, and t_2 to t_3). In the case of annual hourly simulations, the time intervals are usually set to one hour. Finally, $T_{in,HP}$ can be determined by performing an energy balance on the bore field at the current time step.

Equation 8 can be generalised for n time steps as follows (Yavuzturk and Spitler, 1999):

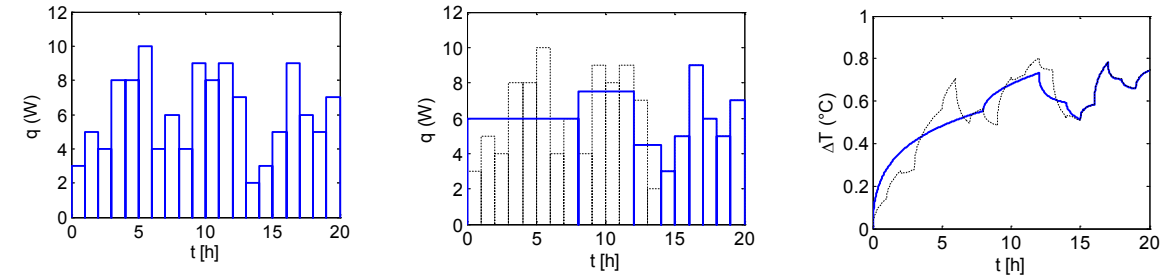
$$T_m = T_g - \sum_{i=1}^{n} \frac{(Q_i-Q_{i-1})}{2\pi k_g L}\, g\left(\frac{t_n-t_{i-1}}{t_s}, \frac{r_b}{H}, \frac{B}{H}, \frac{D}{H}\right) - \frac{Q_n R_b}{L} \quad (9)$$

Solving Equation 9 can be computationally intensive if the number of time steps is large. This is because there is no recurrence in the summation term. In other words, the calculations performed at time step $n-1$ cannot be used at time step n.

4.2 Load aggregation

Load aggregation is typically used to reduce the number of terms in the summation without sacrificing accuracy. It is based on the fact that recent ground loads have a more significant impact on the current mean fluid temperature than distant ground loads. This is illustrated in Figure 7 where ΔT (T_m-T_g) is evaluated using 20 hourly ground loads for a particular bore field and specific ground properties. Figure 7a shows the individual ground loads. In Figure 7b, loads have been aggregated (i.e. averaged) for three time periods; the first 8 hours, then the next four, then the next two. The last 6 hours are kept intact as they have the largest influence on the final value of ΔT. When individual loads are considered, 20 terms are included in the summation to obtain ΔT (Equation 9) while only 9 are included when loads are aggregated. Figure 7c shows the resulting value of ΔT with (solid line) and without (dotted line) aggregation. The predictions of ΔT at t = 12 hours differ as recent loads (4 hours

prior to t = 12 hours) have been averaged in the load aggregation scheme. However, the prediction of ΔT at t = 20 hours is much better (both curves are superimposed) as recent loads (6 hours prior to t = 20 hours) are not aggregated.



a) b) c)

Figure 7: Illustration of the impact of load aggregation: a) individual ground loads; b) aggregated ground loads; c) resulting ΔT with (solid line) and without (dotted line) aggregation.

In the case of hourly simulations, the determination of T_m at the end of a year would require a summation of 8760 terms. One possible alternative would be to aggregate the ground loads of the first 8000 hours, then aggregate the next 730 hours and keep intact the last 30 hours. The summation term would then be reduced to 32 terms. Other aggregation schemes have been proposed by Yavuzturk and Spitler (1999), Bernier et al. (2004), and Liu (2005).

Recent developments regarding the solution of Equation 9 are worth mentioning. Lamarche (2009) has proposed a promising technique which introduces recurrence in the summation term. Pasquier and Marcotte (2008) recognized that the second term on the right hand side of Equation 9 corresponds to a convolution product and suggested to solve it using a spectral approach using fast Fourier transforms which reduces computational time significantly.

5 CONCLUSION

The use of thermal response factors, also known as g-functions, for sizing and simulating ground-coupled heat pump systems is discussed in this paper. In the first part of the paper, thermal response factors are reviewed and an example of their use is presented. Four distinct regions on the g-functions curves are determined. It is also shown that the buried depth of boreholes is important especially for short boreholes and a recommendation is made to introduce a fourth non-dimensional parameter to fully characterize g-functions. Then, the paper suggests a method to use g-functions to size boreholes. The method involves a few iterations in which g-functions are evaluated analytically, using the finite line source, as the solution progresses. With this technique, corrections for r_b/H and interpolation between B/H curves are no longer needed. Finally, the methodology to perform annual simulations of bore fields using g-functions is examined. The concepts of temporal superposition and load aggregation are discussed.

6 ACKNOWLEDEGMENTS

The author would like to thank the graduate students he supervised over the years. Without their efforts this article would not have been possible. The financial support provided by Électricité de France over the years is also gratefully acknowledged. Finally, the Natural Science and Engineering Research Council of Canada funded the author with a discovery grant and through NSERC's Smart Net-Zero Energy Buildings Strategic Research Network.

7 REFERENCES

Ahmadfard, M. and M. Bernier. 2014. “An Alternative to ASHRAE's Design Length Equation for Sizing Borehole Heat Exchangers”, accepted - ASHRAE annual conference, Seattle, June 2014.

ASHRAE. 2011. ASHRAE Handbook-Application. Atlanta: American Society of Heating Refrigeration and Air Conditioning Engineers, Inc.

Baudoin, A. 1988. “Stockage intersaisonnier de chaleur dans le sol par batterie d'échangeurs baionnette verticaux; modèle de prédimensionnement”, Ph.D. Thesis, Université de Reims Champagne-Ardenne, France.

Bernier, M., A. Chahla and P. Pinel. 2008. “Long-term Ground Temperature Changes in Geo-Exchange Systems”, ASHRAE Transactions, 114(2):342-350.

Bernier, M., P. Pinel, R. Labib and R. Paillot. 2004. “A Multiple Load Aggregation Algorithm for Annual Hourly Simulations of GCHP Systems”, Int. J. of Heating, Ventilating, Air-Conditioning and Refrigeration Research, 10(4):471-488.

Bernier, M. 2000. “A Review of the Cylindrical Heat Source Method for the Design and Analysis of Vertical Ground-Coupled Heat Pump Systems”, Fourth international Conference on Heat Pumps in Cold Climates, Aylmer, Québec, August 2000.

Cimmino, M. and M. Bernier. 2014. “A semi-analytical method to generate g-functions for geothermal bore fields”, Int. J. Heat Mass Transfer, 70(c):641-650.

Cimmino, M. and M. Bernier. 2013. "Preprocessor for the generation of g-functions used in the simulation of geothermal systems", Proceedings of the 13th International IBPSA conference, 25-28 August, Chambery, France, pp.2675-2682.

Cimmino. M., M. Bernier and F. Adams. 2013. “A contribution towards the determination of g-functions using the finite line source”, Applied Thermal Engineering, 51(1-2):401-412.

Claesson, J. 2013. Personal communication.

Claesson, J. and S. Javed. 2011. “An analytical method to calculate borehole fluid temperatures for time-scales from minutes to decades”, ASHRAE Transactions, 117(2):279-288.

Cooper, L.Y. 1976. “Heating of a cylindrical cavity”, International Journal of Heat and Mass Transfer, 19 (1976) 575-577.

Eskilson, P. 1987. “Thermal analysis of heat extraction boreholes”, Ph.D. Thesis. University of Lund, Sweden, 264 pp.

Eskilson, P. 1986. “Superposition Borehole Model: Manual for Computer Code”, University of Lund, Lund, Sweden, 104 pp.

Fisher, D.E., S.J. Rees, S.K. Padhmanabhan, and A. Murugappan. 2006. “Implementation and validation of ground-source heat pump system models in an integrated building and system simulation environment”, HVAC&R Research, 12:693-710.

Lamarche L. 2009. “A fast algorithm for the hourly simulations of ground-source heat pumps using arbitrary response factors”, Renewable Energy, 34(10):2252-2258.

Lamarche, L. and B. Beauchamp. 2007, “A new contribution to the finite line-source model for geothermal boreholes”, Energy and Buildings, 39(2):188-198.

Liu, X. 2008. “Enhanced Design and Energy Analysis tool for geothermal water loop heat pump systems”, 9th International IEA Heat Pump Conference, 20 – 22 May 2008, Zürich, Switzerland, paper 4.54.

Liu, X. 2005. “Development and Experimental Validation of Simulation of Geothermal Snow Melting Systems for Bridges”, Ph.D. Thesis, Oklahoma State University, Stillwater, OK, USA.

Hellström, G. and B. Sanner. 1994. “Software for dimensioning of deep boreholes for heat extraction”, in: Proceedings of Calorstock 1994, Espoo/Helsinki, Finland, 195-202.

Marcotte, D. and P. Pasquier. 2008. “Fast Fluid and Ground Temperature Computation for geothermal Ground-Loop Heat Exchanger Systems”. Geothermics, 37(6):651–665.

Philippe, M., M. Bernier and D. Marchio. 2010. “Sizing Calculation Spreadsheet:Vertical Geothermal Bore fields”, ASHRAE Journal, 52(7):20-28.

Philippe, M., M. Bernier and D. Marchio. 2009. “Validity ranges of three analytical solutions to heat transfer in the vicinity of single boreholes”, Geothermics, 38(4):407-413.

Spitler, J.D. 2000. “A design tool for commercial building loop heat exchangers”, in: Fourth International Heat Pumps in Cold Climates Conference, Aylmer, Québec, 2000.

Yavuzturk, C. and J.D. Spitler. 1999. “A short time step response factor model for vertical ground loop heat exchangers”, ASHRAE Transactions 105(2): 475-485.